

Fishtail effect and vortex dynamics in LiFeAs single crystals

A. K. Pramanik, L. Harnagea, C. Nacke, A. U. B. Wolter, S. Wurmehl, V. Kataev, and B. Büchner
Institute for Solid State Research, IFW Dresden, D-01171 Dresden, Germany

We investigate the fishtail effect, critical current density (J_c) and vortex dynamics in LiFeAs single crystals. The sample exhibits a second peak (SP) in the magnetization loop only with the field \parallel c -axis. We calculate a reasonably high J_c , however, values are lower than in ‘Ba-122’ and ‘1111’-type FeAs-compounds. Magnetic relaxation data imply a strong pinning which appears not to be due to conventional defects. Instead, its behavior is similar to that of the triplet superconductor Sr_2RuO_4 . Our data suggest that the origin of the SP may be related to a vortex lattice phase transition. We have constructed the vortex phase diagram for LiFeAs on the field-temperature plane.

PACS numbers: 74.25.Ha, 74.25.Sv, 74.25.Wx

The fishtail effect or the anomalous second peak (SP) in field (H) dependent magnetization (M) loops has been a subject of intense research topic in the field of superconductors with both low and high transition temperatures (T_C).^{1–13} This phenomenon is realized with the enhanced irreversibility in isothermal $M(H)$ or, equivalently, the enhanced critical current density (J_c) at high fields apart from the central peak which occurs around zero field. In type-II superconductors, the magnetic fields above the lower critical field (H_{c1}) penetrate the bulk of the sample in the form of flux lines or vortices. Different mechanisms based on the vortex dynamics have been discussed to explain the SP in high- T_C cuprates which include inhomogeneity of the sample,^{2,3} matching effect,⁴ surface barriers,⁵ geometrical effects,⁶ dynamic effects,⁷ structural phase transition in the vortex lattice (VL),⁸ vortex order-disorder phase transition,^{9–12} crossover from elastic to plastic creep,¹³ etc. However, in spite of plenty of studies dealing with this phenomenon, the general understanding lacks a converging trend and the proposed models appear to be more sample specific.

The recent discovery of superconductivity (SC) in Fe-based pnictides¹⁴ has renewed the interest in vortex dynamics. Similar to cuprates, pnictides are also layer-based superconductors, and exhibit a high T_C and type-II nature. In contrast, pnictides have less anisotropy and larger coherence length (ξ), thus raising question how these influence the vortex dynamics in these materials. The appearance of a SP in $M(H)$ is not an universal phenomenon in different families of pnictides. For the ‘122’ family (AFe_2As_2 , A = Ba, Sr, Ca, etc.) the appearance of a SP is sensitive enough to the compositional elements. The pronounced SP has been observed, for example, in both hole- and electron-doped Ba-122 compounds, which has been ascribed to various mechanisms,^{15–21} but it remains absent in doped Ca-122 compounds.²² Similarly, a SP is not consistently seen in the ‘1111’ (REFeAsO , RE = La, Nd, Ce, Sm, etc.) and in the ‘11’ (FeTe) families.^{23–25} However, to the best of our knowledge the vortex dynamics have not been studied in the ‘111’ family (AFeAs , A = Li, Na, etc) up to now.

Here we study the fishtail effect and the vortex dynamics in single crystals of LiFeAs which belong to the

111 family of pnictides. LiFeAs is an oxygen free compound where superconducting active FeAs layers are separated by Li atoms along the c -axis.²⁶ Remarkably, LiFeAs exhibits SC in absence of any notable Fermi surface nesting and static magnetism,²⁷ however, the presence of antiferromagnetic fluctuations in the normal state is inferred from the nuclear magnetic resonance (NMR) measurements.²⁸ Interestingly, recent experimental NMR results²⁹ and also theoretical calculations^{30,31} indicate a possible p -wave SC state in LiFeAs, which is significantly different from other families within pnictides. As LiFeAs is nonmagnetic and does not require any chemical doping to become superconducting, therefore the FeAs layers are more homogeneous and the crystal is devoid of coexisting magnetic phases which make it an ideal playground to study the vortex dynamics. Based on the sharpness of the rocking curve, recent small angle neutron scattering (SANS) measurements have revealed that that VL in LiFeAs exhibits no long range order, however, better ordering than the doped Ba-122 compounds.^{18,20,32}

We have investigated the properties of the vortex state in LiFeAs by means of isothermal $M(H)$ and magnetic relaxation measurements which are the most extensively used tools for a variety of superconducting materials.^{33,34} Our results imply a pronounced SP in both $M(H)$ and $J_c(H)$ at low temperatures (T) with the applied field parallel to the c -axis. We do not find a SP with $H \parallel ab$ plane. We determine the J_c which is reasonably high, however, lower than those for doped Ba-122 and 1111 compounds. The magnetic relaxation data, on the other hand, imply a nonlogarithmic time (t) dependence with the estimated normalized magnetic relaxation rate (S) being very low (even lower than in Ba-122 and 1111 compounds) signifying a strong pinning for LiFeAs. This specific behavior of the magnetic relaxation is similar to those of triplet superconductors, i.e., Sr_2RuO_4 .³⁵ Our data also indicate that the SP in LiFeAs may be due to a VL phase transition. From the $M(H)$ plots we have constructed the vortex phase diagram on the H - T plane for LiFeAs.

Single crystals of LiFeAs have been grown using the self-flux method as detailed in Ref. 36. The good quality and homogeneity of the crystals are confirmed by an exceptionally small nuclear quadrupole resonance

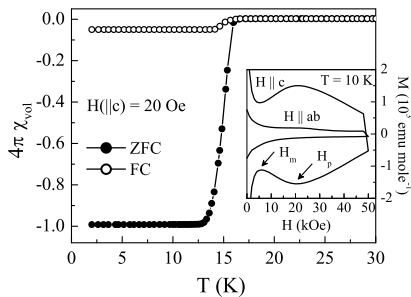


FIG. 1: Temperature dependence of χ_{vol} for LiFeAs deduced from dc- M measured following ZFC and FC protocols. The data have been collected in $H||c = 20$ Oe. The inset shows M vs H plots measured at 10 K with the field parallel to both c -axis and ab -plane.

(NQR) linewidth of 64 kHz, a very low residual resistance of 0.025 m Ω cm and a sharp transition in specific heat data.^{36,37} For the present studies, two crystals ($S1$ and $S2$) of the same batch with rectangular shape have been selected. For the magnetic hysteresis loop sample $S1$ ($3.53 \times 2.5 \times 0.21$ mm³) and for the magnetic relaxation measurements sample $S2$ ($2.89 \times 2.16 \times 0.38$ mm³) have been used. Magnetization have been measured in a Quantum Design MPMS-XL SQUID. Adequate care has been taken to avoid the exposure of the sample to air before mounting it in the magnetometer. All the $M(H)$ and $M(t)$ measurements have been performed after cooling the sample in zero magnetic field from much above T_C to the specific temperature. The $M(H)$ loops have been investigated with the field up to 50 kOe. For the relaxation measurements, the magnetization has been measured as function of time for about 8000 s.

The main panel of Fig. 1 presents the temperature dependence of the volume susceptibility (χ_{vol}) measured following the zero-field-cooled (ZFC) and field-cooled (FC) protocols for magnetization measurements. χ_{vol} has been deduced from the measured dc- M with a field of 20 Oe applied parallel to the crystallographic c -axis. The data has been corrected for demagnetization effects.³⁸ It is evident from Fig. 1 that the sample exhibits bulk SC as characterized by the diamagnetic signal at low T . The sharp transition as well as the high value of χ_{vol} in M_{ZFC} demonstrate the high quality of our crystal. We determine T_C from the bifurcation point between ZFC and FC branches of the magnetization to be around 16.5(5) K. In the inset of the Fig. 1 we have plotted the $M(H)$ data at 10 K with H parallel to both c -axis and ab -plane. With increasing H for $H||c$, the magnetic irreversibility (M_{irr}) initially decreases showing a minimum at a field H_m . On further increase in H , M_{irr} increases and exhibits a peak (SP) at a field H_p . However, we do not find any trace of a SP for $H||ab$ -plane. While this significant anisotropic behavior in appearance of the SP is similar to other pnictide superconductors,¹⁵ but it remains different from cuprates, i.e., $\text{La}_{1-x}\text{Sr}_x\text{CuO}_4$.¹²

Since the SP in $M(H)$ is only evident for $H||c$ in this

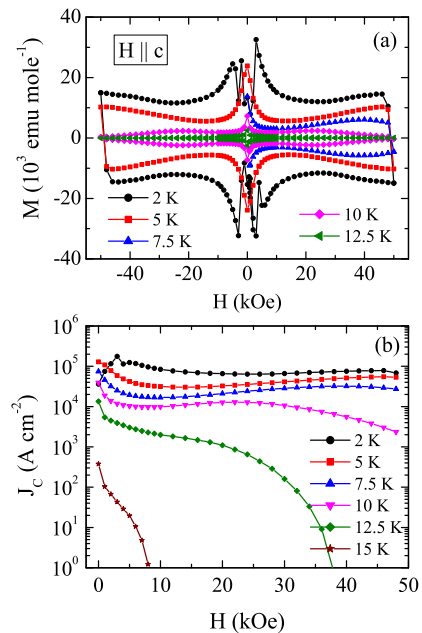


FIG. 2: (Color online) (a) The isothermal M vs H loops recorded at different temperatures with $H||c$ for LiFeAs. (b) The critical current J_c as calculated from the $M(H)$ loops in (a) as function of field for different temperatures; for details see text.

compound, we have collected the $M(H||C)$ isotherms at different T within the SC regime in order to understand the SP characteristics. The data are plotted in Fig. 2a where M vs H loops are quite symmetric with respect to both the sweeping direction as well as the polarity of the magnetic field. At low T , however, even though the onset of the SP is evident, the SP cannot be observed within the measurable field range. Interestingly, $M(H)$ at 2 K exhibits irregular jumps close to $H = 0$. These jumps are commonly known as ‘flux jump’ effects³⁹ and will be presented elsewhere in more detail. With the increase in T , a clear SP can be observed in the $M(H)$ loops. Moreover, we find a field H_{irr} above which M_{irr} in data vanishes. With increasing T , all the characteristic fields, i.e., H_m , H_p and H_{irr} decrease, and their T variation will be discussed in a later section.

From the magnetic irreversibility in $M(H)$ we have calculated the critical current J_c exploiting the Bean’s critical state model⁴⁰ $J_c = 20\Delta M/[a(1 - a/3b)]$, where $\Delta M = M_{dn} - M_{up}$, M_{up} and M_{dn} are the magnetization measured with increasing and decreasing field, respectively, and a and b ($b > a$) are the dimensions of the crystal perpendicular to the applied H . The unit of ΔM is in emu/cm³, a and b are in cm and the calculated J_c is in A/cm². The calculated $J_c(H)$ has been plotted in Fig. 2b for different T . The variation in $J_c(H)$ is nonmonotonic and exhibits a broad peak (SP) in the high field region, which is in line with ΔM in Fig. 2a. At low T , J_c is rather high, however, its value still being lower than in doped Ba-122 and 1111 compounds where $J_c \sim 10^6$ or

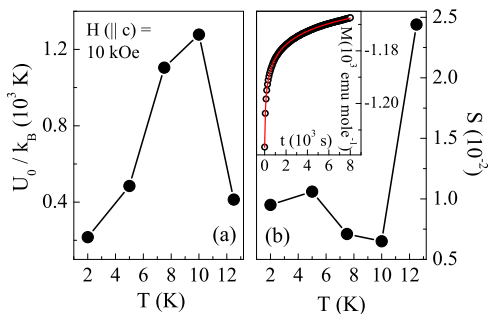


FIG. 3: (Color online) (a) The energy barrier U_0/k_B obtained by fitting of Eq. 1 as a function of temperature. (b) The magnetic relaxation rate S as function of temperature in $H||c = 10$ kOe as calculated using Eq. 2 at $t = 1000$ s. The inset exemplary shows the best fit of the magnetic relaxation data at $T = 10$ K and $H||c = 10$ kOe using Eq. 1.

even higher.^{15–17,19,24} This is in agreement with the level of disorder as revealed from the SANS studies.^{18,20,32}

To understand the origin of the SP and the reasonably high J_c -values in LiFeAs, we have studied detailed vortex dynamics in this compound by means of T - and H -dependent magnetic relaxation measurements.^{33,34} Magnetic relaxation in superconductors is a result of non-equilibrium spatial arrangement of vortices due to pinning sites. External applied magnetic field exerts Lorentz forces on the vortices resulting in their movement, which causes a change in $M(t)$. In contrast to the original Anderson-Kim model,⁴¹ our relaxation data exhibit a nonlogarithmic time dependence and can be best fitted with the interpolation formula:³³

$$M(t) = M_0 \left[1 + \frac{\mu k_B T}{U_0} \ln \left(\frac{t}{t_0} \right) \right]^{-1/\mu}, \quad (1)$$

where k_B is the Boltzmann constant, U_0 is the energy barrier height in absence of a driving force, t_0 is the characteristic relaxation time (usually $\sim 10^{-6}$ s for type-II superconductors), and μ is the field-temperature dependent parameter. This formula yields the normalized magnetic relaxation rate $S [= (1/M)dM/d \ln(t)]$ as:³³

$$S(t) = \frac{k_B T}{U_0 + \mu k_B T \ln(t/t_0)}. \quad (2)$$

Magnetic relaxation has been measured at different T in $H||c = 10$ kOe. We find a very slow relaxation, i.e., there is only a 4% change in magnetic moment at $H = 10$ kOe and $T = 10$ K within a time period of 8000 s which is much lower than that observed in cuprates and 122-pnictides.^{15,33} $U_0/k_B(T)$ and $S(T)$ as extracted from the fitting of the data exploiting Eqs. 1 and 2 are plotted in Fig. 3a and 3b, respectively. One representative fitting of our data has been included as an inset in Fig. 3b. Surprisingly, we find a very high value of t_0 of the order of 10 s, which is orders of magnitude higher than

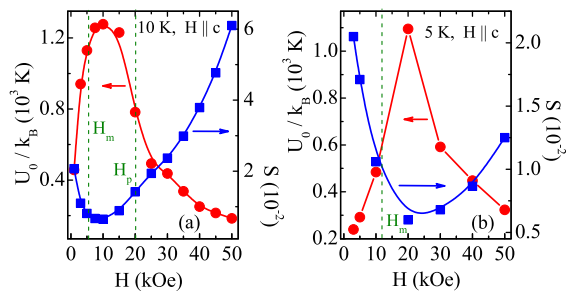


FIG. 4: (Color online) (a) The field dependence of U_0/k_B and S extracted from the magnetic relaxation data at 10 K exploiting Eqs. 1 and 2. The vertical dashed lines mark H_m and H_p ; details see text. (b) The same physical properties U_0/k_B and S shown for 5 K.

for other families in pnictides and cuprates.^{15,22,33,34} For LiFeAs the value for the energy barrier U_0/k_B increases with T , however, above 10 K it drops down due to larger thermal fluctuations. A similar behavior can be detected for $S(T)$, which also shows a non-monotonous behavior (calculated at $t = 1000$ s) with a steep decrease followed by an increase upon lowering temperature.

In addition to the temperature dependent relaxation studies, $M(t)$ has been measured in different fields ($H||c$) along the hysteresis loop at constant T . Similarly, we have extracted U_0/k_B and S using Eqs. 1 and 2. Fig. 4a presents the results for $U_0/k_B(H)$ and $S(H)$ at 10 K. Here, the vertical dashed lines in Fig. 4a represent the minimum and maximum (SP) in $M(H)$ at 10 K (see Fig. 1 and 2). It is evident from the plot that U_0/k_B initially increases with applied fields and then decreases, showing a peak at a field in between H_m and H_p , where the related calculated $S(H)$ exhibits a minimum. This variation in $S(H)$ is similar to doped Ba-122 compounds.^{15,21} To examine the behavior of $U_0/k_B(H)$ and $S(H)$ at low- T where the SP shifts significantly to higher field values, we have calculated the parameters at 5 K following the same method. Our results show that although the field, where U_0/k_B (S) exhibits a maximum (minimum), increases from ≈ 10 kOe at 10 K to ≈ 20 kOe at 5 K (Fig. 4b), this variation does not scale with the large increase in H_p at low T (see Fig. 2a). Note, that the calculated S in Figs. 3 and 4 is very low, and that the values even go below those for Ba-122 and 1111 compounds, where $S > 0.01$.^{15,21,23,24} The low value of S paired with our very high t_0 -value imply a high pinning in LiFeAs. This is quite intriguing as J_c in LiFeAs is lower than in Ba-122 and 1111 materials,^{15–17,19,24} which means that other type of pinnings rather than the conventional defects are active in LiFeAs. Indeed, our crystal is of good quality and homogeneous as discussed earlier. However, such slow magnetic relaxation has been observed in the p -type superconductor Sr_2RuO_4 ($S \sim 10^{-3}$), where it has been pointed out that the observed strong pinning is related to the superconducting phase of triplet nature rather than conventional defects.³⁵ This raises the question if the ob-

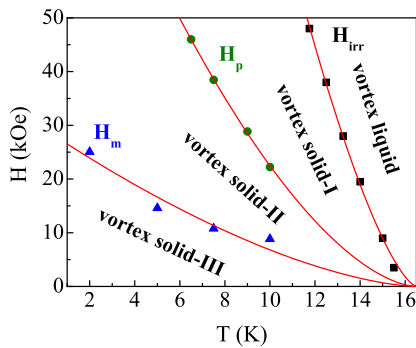


FIG. 5: (Color online) The vortex phase diagram on the H - T plane with $H||c$ for LiFeAs. Solid lines represent fits of the data using the functional form $H_x(T) = H_x(0)(1 - T/T_C)^n$ (see text).

served low S -value in combination with the observed J_c in our single crystal of LiFeAs might be within the lines of other studies, which recently proposed triplet pairing in LiFeAs,^{29–31} but this requires further detailed investigations in the future.

From the so far obtained data we have constructed the vortex phase diagram on the H - T plane for LiFeAs (Fig. 5). Above H_{irr} , vortices are in a liquid state. Below H_{irr} , they are in a solid state, however, its nature changes between different field regimes indicated in the figure (named I, II and III). All the characteristic fields show a strong T dependence where the data can be fitted well with the functional form $H_x(T) = H_x(0)(1 - T/T_C)^n$. We obtain $H_{irr}(0) = 299.5(9)$ kOe and $n = 1.46(4)$, $H_p(0) = 105.7(8)$ kOe and $n = 1.66(3)$, $H_m(0) = 29.1(4)$ kOe and $n = 1.56(3)$. The values of the exponent n are reasonably consistent with those for other pnictides.^{15,16,23,24}

Now we discuss the origin of the SP effect and the intriguing vortex dynamics in LiFeAs. The strong T dependence of the transition lines (Fig. 5) discards the possibility that the SP in LiFeAs arises due to a vortex order-disorder phase transition.^{9–12} Moreover, an absence of 'mirror-image' correlation between $M(H)$ and $S(H)$ in Figs. 2 and 4 imply that the dynamic model⁷ is not valid in the present case. Although, the nature of $U_0/k_B(H)$ in Fig. 4 has qualitative similarity to the model which predicts the SP being associated with a crossover in flux dynamics from elastic ($< H_p$) to plastic ($> H_p$) creep with increasing field,¹³ the peak in

$U_0/k_B(H)$ for LiFeAs occurs much below the SP, and in low- T at 5 K this mismatch increases. Moreover, this model predicts $H_p \propto [1 - (T/T_C)^4]^{1.4}$ which does not describe the present $H_p(T)$ dependence shown in Fig. 5. Henceforth, the validity of this model for LiFeAs is questionable.

On the other hand, a structural phase transition in the VL is also an attractive and possible model which argues that the SP is associated with the transformation of a hexagonal VL to a square one with field.⁸ The square structure is supported by the fourfold symmetry of the intervortex interaction which can originate in various situations, like, for the anisotropic (d -wave) nature of the superconducting gap as in $\text{La}_{2-x}\text{Sr}_x\text{CuO}_4$,⁴² for materials with low Ginzburg-Landau (GL) parameters (κ) as in $\text{YNi}_2\text{B}_2\text{C}$,⁴³ in the extended GL theories with more than one order parameter as for the p -wave superconductor Sr_2RuO_4 ,⁴⁴ etc. Recently, such scenario of a structural phase transition in the VL has been proposed in $\text{Ba}(\text{Fe}_{0.925}\text{Co}_{0.075})_2\text{As}_2$ where a minimum in $S(T)$ and $S(H)$ has been found.²¹ Altogether, taking into account a similar behavior with a minimum in $S(T)$ and $S(H)$ in LiFeAs, paired with a comparatively low value of κ (≈ 30)³² and the proposed p -wave SC^{29–31} in LiFeAs, a structural phase transition in the VL is a possible scenario for the existence of the SP in this compound. However, further investigations including microscopic probes are required to confirm these observations.

In summary, single crystalline LiFeAs exhibits a SP in the $M(H)$ loop with $H||c$ -axis. The calculated J_c s are reasonably high, however, the values are lower than in the doped Ba-122 and 1111 compounds. We find an extraordinary slow magnetic relaxation implying a strong pinning which appears not to be related to conventional defects. Instead, the behavior of magnetic relaxation is similar to the p -wave superconductor Sr_2RuO_4 . We have constructed the vortex phase diagram on the H - T plane for LiFeAs, with the characterized fields H_{irr} , H_p and H_m showing a strong T dependence. In accordance with recent investigations on $\text{Ba}(\text{Fe}_{0.925}\text{Co}_{0.075})_2\text{As}_2$ our data imply that the SP in LiFeAs most likely originates from a VL phase transition. Nonetheless, further studies involving microscopic probes are required to comprehend the SP and vortex dynamics in this compound.

This work has been supported by the DFG through SPP 1458 and Grant No. Be1749/13 and WO1532/1-1.

¹ S. B. Roy and P. Chaddah, *Physica C* **279**, 70 (1997).

² M. Daeumling *et al.*, *Nature* **346**, 332 (1990).

³ L. Klein *et al.*, *Phys. Rev. B* **49**, 4403 (1994).

⁴ R. Yoshizaki *et al.*, *Physica C* **225**, 299 (1994).

⁵ V. N. Kopylov *et al.*, *Physica C* **170**, 291 (1990).

⁶ Y. V. Bugoslavsky *et al.*, *Physica C* **233**, 67 (1994).

⁷ L. Krusin-Elbaum *et al.*, *Phys. Rev. Lett.* **69**, 2280 (1992).

⁸ B. Rosenstein and A. Knigavko, *Phys. Rev. Lett.* **83**, 844

(1999).

⁹ B. Khaykovich *et al.*, *Phys. Rev. Lett.* **76**, 2555 (1996).

¹⁰ D. Ertas and D. R. Nelson, *Physica C* **272**, 79 (1996).

¹¹ D. Giller *et al.*, *Phys. Rev. Lett.* **79**, 2542 (1997).

¹² Y. Radzyner *et al.*, *Phys. Rev. B*, **65**, 214525 (2002).

¹³ Y. Abulafia *et al.*, *Phys. Rev. Lett.* **77**, 1596 (1996).

¹⁴ Y. Kamihara *et al.*, *J. Am. Chem. Soc.* **130**, 3296 (2008).

¹⁵ R. Prozorov *et al.*, *Phys. Rev. B* **78**, 224506 (2008).

- ¹⁶ B. Shen *et al.*, Phys. Rev. B **81**, 014503 (2010).
¹⁷ D. L. Sun *et al.*, Phys. Rev. B **80**, 144515 (2009).
¹⁸ M. R. Eskildsen *et al.*, Phys. Rev. B **79**, 100501(R) (2009).
¹⁹ H-J. Kim *et al.*, Phys. Rev. B **79**, 014514 (2009).
²⁰ D. S. Inosov *et al.* Phys. Rev. B **81**, 014513 (2010).
²¹ R. Kopeliansky *et al.*, Phys. Rev. B **81**, 092504 (2010).
²² A. K. Pramanik *et al.*, Phys. Rev. B **82**, 014503 (2010).
²³ H. Yang *et al.*, Phys. Rev. B **78**, 092504 (2008).
²⁴ D. Bhoi *et al.*, arXiv:1002.0208.
²⁵ T. Taen *et al.*, Phys. Rev. B **80**, 092502 (2009).
²⁶ J. H. Tapp *et al.*, Phys. Rev. B **78**, 060505(R) (2008).
²⁷ S.V. Borisenko *et al.*, Phys. Rev. Lett. **105**, 067002 (2010).
²⁸ P. Jeglič *et al.*, Phys. Rev. B **81**, 140511(R) (2010).
²⁹ S.-H. Baek *et al.*, (unpublished).
³⁰ L. Hozoi and P. Fulde, Phys. Rev. Lett. **102**, 136405 (2009).
³¹ P. M. R. Brydon *et al.* arXiv:1009.3104
³² D. S. Inosov *et al.*, Phys. Rev. Lett. **104**, 187001 (2010).
³³ Y. Yeshurun *et al.*, Rev. Mod. Phys. **68**, 911 (1996).
³⁴ G. Blatter *et al.*, Rev. Mod. Phys. **66**, 1125 (1994).
³⁵ E. Dumont and A. C. Mota, Phys. Rev. B **65** 144519 (2002).
³⁶ I. Morozov *et al.*, Crystal Growth and Design (In press) (DOI: 10.1021/cg1005538).
³⁷ U. Stockert *et al.*, (unpublished).
³⁸ J. A. Osborn, Phys. Rev. **67**, 351 (1945).
³⁹ M. E. McHenry *et al.*, Physica C **190**, 403 (1992).
⁴⁰ C. P. Bean, Phys. Rev. Lett. **8**, 250 (1962); Rev. Mod. Phys. **36**, 31 (1964).
⁴¹ P. W. Anderson and Y. B. Kim, Rev. Mod. Phys. **36**, 39 (1964).
⁴² R. Gilardi *et al.*, Phys. Rev. Lett. **88**, 217003 (2002).
⁴³ D. McK. Paul, Phys. Rev. Lett. **80**, 1517 (1998).
⁴⁴ T. M. Riseman *et al.*, Nature **396**, 242 (1998).